Energy Engineering

Tech Science Press

DOI: 10.32604/EE.2021.016107

ARTICLE

Impacts of Torrefaction on PM_{10} Emissions from Biomass Combustion

Zihao Wang, Dunxi Yu*, Jingkun Han and Jianqun Wu

State Key Laboratory of Coal Combustion, Huazhong University of Science and Technology, Wuhan, 430074, China

*Corresponding Author: Dunxi Yu. Email: yudunxi@hust.edu.cn

Received: 06 February 2021 Accepted: 06 May 2021

ABSTRACT

Typical biomass torrefaction is a mild pyrolysis process under conditions of ordinary pressure, low temperature (200–300°C) and inert atmosphere. Torrefaction is considered to be a competitive technology for biomass pretreatment, but its impacts on the emissions of particulate matter from biomass combustion are worthy of further study. In this paper, three kinds of biomass, i.e., bagasse, wheat straw and sawdust were selected for torrefaction pretreatment and the impacts of torrefaction on the emission characteristics of PM_{10} from biomass combustion were investigated. The combustion experiments were carried out on a drop tube furnace. The combustion-generated particulate and bulk ash samples were collected and subjected to analyses by various techniques. The results show that torrefaction tends to result in a reduction of PM_1 (particulates with an aerodynamic diameter less than 1 μm) emissions from combustion, but the extent of reduction is dependent on biomass type. The reduction of PM_1 from the combustion of torrefied biomass is mainly because that the torrefaction process removes some Cl and S from the biomass, thereby suppressing the release of alkali metals and the emissions of PM_1 during the combustion process. As for PM_{1-10} (particulates with an aerodynamic diameter within 1–10 μm), its emissions from combustion of torrefied biomasses are consistently reduced, compared with their untreated counterparts. This observation is primarily accounted for the enhanced particle coalescence/agglomeration in combustion of torrefied biomasses, which reduces the emissions of PM_{1-10}.

KEYWORDS

Biomass; combustion; torrefaction; particulate matter

1 Introduction

Coal still accounts for a significantly high proportion (>50%) in China's energy structure. Its energy utilization has caused adverse impacts on the ecological environment and human health, and the pursuit of new alternative energy has become a hot topic [1]. Biomass, with a huge global reserve, is considered as renewable carbon neutral energy [2,3]. Its utilization in the power sector has attracted significant attention [4].

Combustion is considered the most direct way to obtain energy from biomass [5]. However, biomass has many shortcomings in the direct combustion process. In terms of physical properties, biomass has high moisture content, poor grindability and low energy density, which limits its large-scale utilization. On the other hand, biomass usually contains high contents of AAEMs (alkali and alkali earth metals), Cl and S [6], which may aggravate the ash-related problems in the process of combustion. Meanwhile, the

emissions of particulate matter, especially PM_{10} (particulates with an aerodynamic diameter less than 10 μm), are the main factor in the formation of haze. Therefore, pretreatment has often been adopted for the improvement of biomass quality, and to facilitate its large-scale utilization.

As a promising pretreatment technology of biomass, torrefaction can significantly improve its calorific value, hydrophobicity, grindability and other characteristics through pyrolysis of raw biomass in an inert atmosphere at 200–300°C [7–9]. The moisture content of the torrefied biomass is usually below 3%, and the low heating value is usually above 15 MJ/kg. Meanwhile, the grindability of the torrefied biomass is close to that of some kinds of coal. The improvements of the characteristics of torrefied biomass reduce the cost of biomass utilization and improve the combustion stability. In addition, numerous studies [10–12] have shown that Cl, S and other elements in biomass will migrate and be released to a certain extent during the torrefaction process. These changes caused by torrefaction process are likely to affect the emission characteristics of PM_{10} during torrefied biomass combustion.

In the existing literatures, focuses on the impacts of torrefaction on PM_{10} emission during biomass combustion are limited. Wang et al. [13] compared PM_{10} emission from raw rice straw and torrefied rice straw (300°C). It was found that $PM_{0.3}$, $PM_{0.3–1}$ and $PM_{1–10}$ produced by the torrefied rice straw were reduced by 55%, 55% and 16%. Yani et al. [14] studied the emission behaviors of PM_{10} from the combustion of raw and torrefied mallee leaf (220, 250, 280°C). It was found that the amount of PM_1 produced by the torrefied mallee leaf decreased. Han et al. [15] found that torrefaction promoted the migration of alkali metals to PM_{1+} in the process of the combustion of torrefied rice husk (270°C), which led to the decrease of the yields of PM_1. These investigations are often limited to single biomass. Considering the great differences in the composition of different types of biomass [16], it is quite necessary to test the generalization of the conclusions obtained with a wider range of biomasses in the same reaction system.

This paper selected three biomasses of common interest for the investigation: bagasse (hereafter denoted as BG), wheat straw (hereafter denoted as WS) and sawdust (hereafter denoted as SD). They were torrefied at 270°C after being crushed and screened. The torrefied samples were termed as TBG, TWS and TSD, respectively. The raw and torrefied samples were combusted in a drop tube furnace (DTF). The particulate matter and the bulk ash samples were collected for subsequent analysis. By characterizing the particle size distribution, element composition and particle morphology, the effects of torrefaction on the emission characteristics of PM_{10} from biomass combustion were explored. The underlying mechanisms were elucidated.

2 Experimental

2.1 Sample Preparation and Torrefaction Tests

The torrefaction experiment was carried out in a fixed-bed reactor. It consists of air intake section, temperature control section, heating section and water-cooling section. Before the torrefaction experiment, the raw biomass was first ground by a knife mill and sieved to below 100 μm. The raw biomass was placed in a covered porcelain boat and the porcelain boat was placed in a calibrated constant temperature zone of the fixed-bed reactor with N_2 continuously introduced at a flow rate of 3 L/min to ensure an inert atmosphere in the reactor. The temperature of the reactor was raised to 270°C at a heating rate of 15 °C/min, and kept at 270°C for 30 min. Then the porcelain boat was taken out and placed in a N_2-flowed container to quench to room temperature. The mass yields of the residue solids from the torrefaction of BG, WS and SD were 75.5%, 72.5%, and 81.3%, respectively.

2.2 Sample Analyses

Proximate analysis of samples was performed according to the standard GB/T 28731-2012. Ultimate analysis was performed according to standard ASTM D5373, and the composition of ash was measured by X-Ray Fluorescence Spectrometry (XRF). In view of the obvious contents of AAEMs in each sample, and the important role they played in the emissions of PM_{10}, the raw and torrefied samples were all

digested by a mixed solution of nitric acid, hydrogen peroxide and hydrofluoric acid, and then the mixed solution was analyzed by Inductively Coupled Plasma-Mass Spectrometry (ICP-MS) to perform quantitative analysis of AAEMs. The results will be discussed below.

2.3 Combustion Tests and Sample Analysis

The combustion tests of raw and torrefied biomass were carried out in a drop tube furnace whose configuration has been detailed elsewhere [17]. The drop tube furnace system consists of feeding section, reaction section, air inlet section and temperature control section. The feeder is a vibrating powder feeder produced by Sanki. The reaction tube of this system is a corundum tube with a length of 2000 mm and an inner diameter of 56 mm. The furnace body of this system is heated by a silicon carbide rod and the length of the constant temperature zone of the furnace body is 1500 mm. The air inlet section is composed of a gas cylinder, a pressure reducing valve and a mass flowmeter. According to the actual combustion temperature of the pulverized coal furnace and at the same time providing a reference for the study of co-firing of biomass and coal, the experimental temperature was set at 1300°C. The experimental atmosphere was air with a flow rate of 10 L/min. The samples were fed into the furnace at a rate of 0.1 g/min, and the residence time of samples in the furnace was about 2 s. The flue gas generated by combustion was extracted by a vacuum pump and passed through a sampling tube with water cooling and N_2 quenching to avoid secondary reactions. The particles from combustion were collected by a cyclone separator and a Dekati Low Pressure Impactor (DLPI) with a heating system. The temperature of the heating system was set to 135°C to prevent the acid condensation [18]. Particles with aerodynamic diameter larger than 10 μm (PM_{10+}) were collected by the cyclone separator. Particles collected by DLPI were defined as PM_{10}, and separated into 14 stages of which the particles collected at Stages 1–8 were corresponded to PM_1 and those at Stages 9–14 were corresponded to PM_{1-10}. The experiments of each condition were conducted at least 3 times to ensure data accuracy. The bulk ash from combustion was collected by fiberglass filters. The particle collection experiments and the bulk ash collection experiments were carried out separately. The particle size distributions of PM_{10} were obtained by weighing the particles collected in each stage of DLPI with an electronic balance (accuracy of 0.001 mg). The composition and microscopic morphology of particles and bulk ash were characterized by Scanning Electron Microscope with an Energy Dispersive Spectrometer (SEM-EDS).

3 Result and Discussion

3.1 Properties of the Torrefied Biomass

Tab. 1 shows the basic fuel properties of the raw and torrefied biomass. Compared with BG, WS and SD, the contents of volatile matter and moisture of TBG, TWS and TSD are significantly reduced, and the mole ratio of C/H and C/O increases by 23%, 27%, 19% and 24%, 36%, 22%, respectively. This means that there will be less energy loss during the combustion of torrefied biomass. According to the formula: element release rate = 1–(element content of torrefied sample *mass yield)/(element content of raw sample), it can be calculated that N is basically not released during torrefaction process. S is released by 50%, 54%, 49% and Cl is released by 67%, 5%, and 19%, respectively. In view of the fact that the presence of Cl and S can promote the release of alkali metals and the generation of particulate matter during combustion, the release of Cl and S in the torrefaction process is likely to affect the generation of particulate matter during combustion process.

From the analysis of ash composition, it shows that the main component of BG and TBG ashes is SiO_2 (about 60%). The WS and TWS ashes contain high levels of SiO_2 (about 40%), K_2O (20%) and CaO (10%). On the other hand, CaO is the most important component of SD and TSD ashes, accounting for about 45%. The many differences of different types of biomass may have important impacts on the generation of PM_{10} from combustion.

Table 1: Fuel properties of different biomasses (ad, wt, %)

Samples	Proximate analysis				Ultimate analysis					
	Ash	Volatile matter	Fixed carbon	Moisture	C	H	O*	N	S	Cl
BG	5.82	75.96	14.24	3.98	45.14	5.76	38.75	0.40	0.15	0.046
TBG	7.17	67.91	24.03	0.89	50.81	5.28	35.20	0.55	0.10	0.020
WS	11.73	68.20	15.27	4.80	40.90	5.55	35.50	1.08	0.44	1.003
TWS	15.39	57.51	25.90	1.20	46.88	5.01	29.92	1.32	0.28	1.310
SD	8.09	72.64	17.01	2.26	44.21	5.63	38.83	0.68	0.30	0.012
TSD	9.87	67.27	22.10	0.76	48.32	5.17	34.76	0.93	0.19	0.012
Samples	Na_2O	MgO	Al_2O_3	SiO_2	P_2O_5	SO_3	Cl	K_2O	CaO	Fe_2O_3
BG	n.a.	3.57	5.53	61.09	5.76	4.40	n.a.	7.71	6.64	5.30
TBG	n.a.	2.98	5.44	58.92	5.57	4.15	n.a.	8.71	7.34	6.89
WS	n.a.	4.10	4.32	41.54	3.19	7.31	9.72	18.57	9.94	1.31
TWS	n.a.	3.37	4.00	37.01	3.16	8.29	11.02	20.35	11.16	1.64
SD	n.a.	4.67	5.66	24.01	4.09	7.88	n.a.	6.36	44.59	2.74
TSD	n.a.	5.65	6.38	17.34	4.70	8.78	n.a.	6.98	47.77	2.40

Note: *:by difference.

3.2 Particle Size Distributions (PSDs), Yields and Element Compositions of PM_{10}

The particle size distributions of PM_{10} are shown in Fig. 1, and the results are based on the ash content of the samples. It can be concluded that the particle size distributions of PM_{10} produced by the combustion of these samples are approximately bimodally distributed, and the dividing point of the fine and coarse modes is around 1 μm, which is consistent with previous studies [19] and also in line with the generation mechanism of PM_{10} [20]. The PM_1 is principally formed by vaporization-condensation, while PM_{1-10} is mainly formed through fragmentation of char and excluded minerals, coalescence/agglomeration of included minerals and ash particles. For BG and TBG, the peaks of the fine mode and coarse mode are located near 0.05 μm and 4.4 μm, respectively (Fig. 1a), but the two peaks of PSDs of TBG are lower than those of BG. On the other hand, the particle size distribution of PM_1 from the combustion of TBG is generally below that from the combustion of BG. For WS and TWS, the fine mode and coarse mode peaks are located around 0.08 μm and 4.4 μm, respectively (Fig. 1b), and the particle size distribution of PM_{1-10} from the combustion of TWS is generally below that from the combustion of WS. The peaks of fine mode and coarse mode of SD and TSD are located around 0.05 μm and 4.4 μm, respectively (Fig. 1c), and the particle size distributions of fine mode are similar as for SD and TSD, while the coarse mode peak decreases significantly for the combustion of TSD.

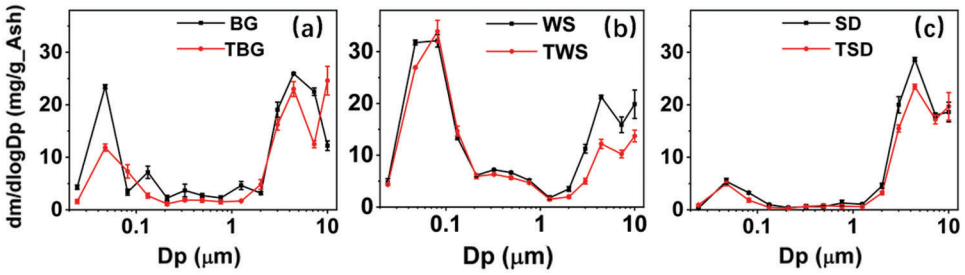

Figure 1: Particle size distributions of PM_{10} from combustion of different biomasses

Due to the different emission mechanisms of fine and coarse modes particles, PM_{10} is divided into PM_1 and PM_{1-10} for further research. Fig. 2 shows the yields of PM_1 and PM_{1-10} based on the ash content to explore the yields capacity of PM_{10} of these samples. The yields of PM_1 and PM_{1-10} from the combustion of BG, WS and SD are 11.4 mg/g_Ash, 24.0 mg/g_Ash, 2.9 mg/g_Ash and 16.1 mg/g_Ash, 12.2 mg/g_Ash, 15.4 mg/g_Ash. Compared with BG, the yields of PM_1 from the combustion of TBG decrease by about 40%. Compared with WS and SD, the yields of PM_1 from the combustion of TWS and TSD also show a decreasing trend, but the reduction degrees are not as obvious as the reduction degree of TBG. In addition, compared with raw biomass, the yields of PM_{1-10} produced by the combustion of torrefied biomass are also reduced to varying degrees. Compared with BG, WS and SD, the yields of PM_{1-10} from TBG, TWS and TSD are reduced by approximately 19%, 40% and 13%, respectively. The result indicates that torrefaction process may promote the coalescence/agglomeration of PM_{1-10} or inhibit the breaking of particles in the combustion process. On the other hand, our group's existing research [13] on the raw and torrefied rice straw showed that compared with raw rice straw, the yields of PM_1 and PM_{1-10} from the combustion of torrefied rice straw (300°C) were also reduced. And our group's existing research [15] on the rice husk also showed that torrefied rice husk produced less amount of PM_1.

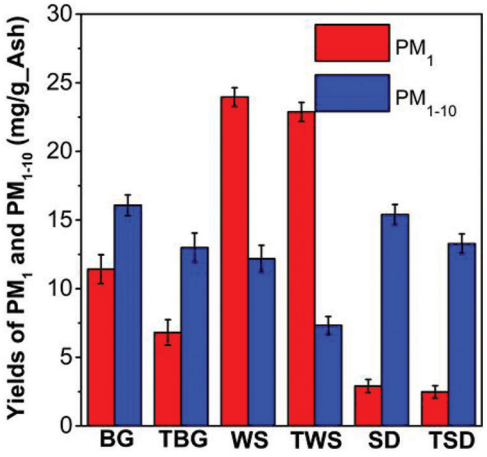

Figure 2: Ash-based yields of PM_1 and PM_{1-10} from combustion of different biomasses

In order to further understand the characteristics of PM_{10} of these samples, the elemental compositions of PM_1, PM_{1-10} and PM_{10+} were tested and characterized, and the results are shown in Fig. 3. The compositions of PM_1 in each sample are mainly composed of easily vaporized elements such as Cl, S, Na and K, which is consistent with the mechanism that PM_1 is mainly formed by the vaporization and condensation of alkali metal salt. For WS and TWS, PM_1 is mainly composed of alkali chlorides. For SD and TSD with low content of Cl and high content of S, PM_1 contains more alkali sulfates. For BG, TBG, WS and TWS, the main elements in PM_{1-10} from combustion are Si, Ca, Fe, and K, while PM_{1-10} from the combustion of SD and TSD mainly contains Ca. The kinds of the main elements of PM_{10+} from the combustion of each sample are similar to those of the corresponding PM_{1-10}. On the other hand, it is worth noting that compared with SD and TSD, the contents of K and Si of PM_{1-10} and PM_{10+} from the combustion of the other four samples are more obvious, which may have an impact on the generation of PM_{1-10}.

3.3 The Impacts of Torrefaction on the Transformation of Elements in PM_{10}

In order to explore the reasons for the different emission characteristics of PM_{10} from the combustion of raw and torrefied biomass, the yields of each element in PM_1 and PM_{1-10} were analyzed and compared. The

results are shown in Fig. 4. At the same time, according to the elemental composition analysis (Fig. 3), it can be concluded that AAEMs, Cl and S play an important role in the generation of PM_{10}. Therefore, quantitative analysis of some of these elements in each sample was carried out. The results based on the ash content are shown in Fig. 5.

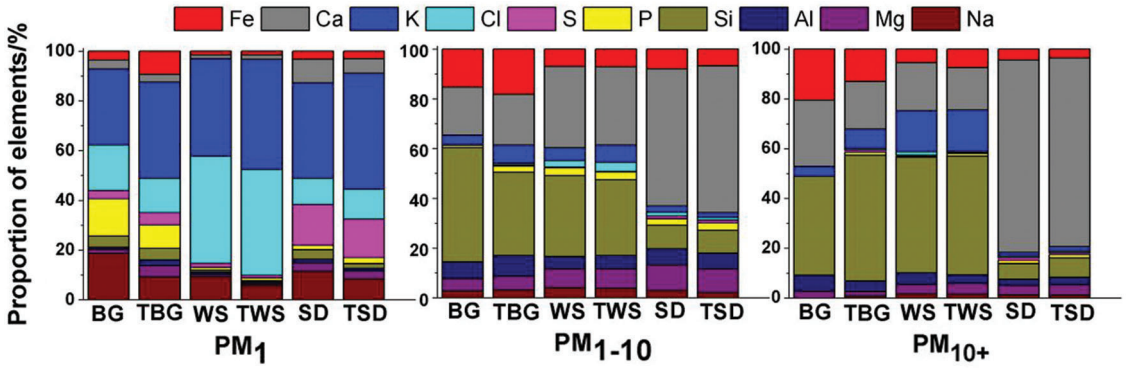

Figure 3: Elemental compositions of PM_1, $PM_{1–10}$ and PM_{10+} from combustion of different biomasses

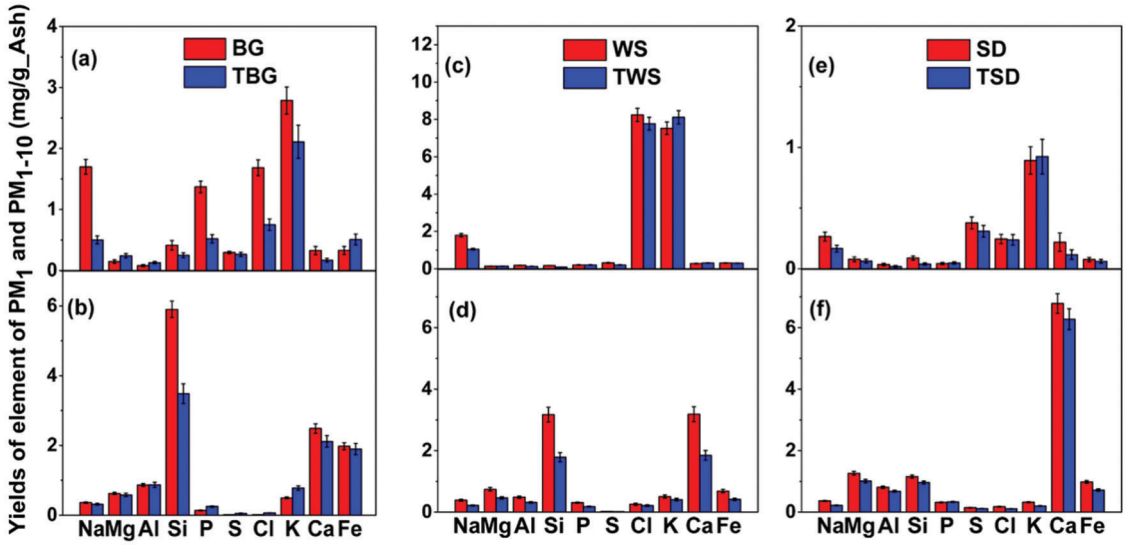

Figure 4: Yields of elements in PM_1 and $PM_{1–10}$ from combustion of different biomasses. (a, c, e) PM_1, (b, d, f) $PM_{1–10}$

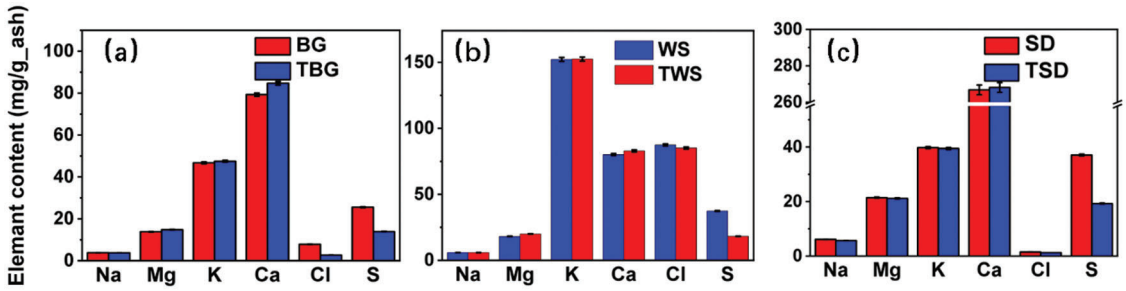

Figure 5: Ash-based contents of major elements in different biomasses

It can be seen from Fig. 4a that compared with BG, the reduction in the yields of PM_1 of TBG is mainly due to the decrease of Na, K, and Cl. Combined with Fig. 5a, the differences between BG and TBG are not much obvious in terms of the contents of K and Na, but the contents of Cl and S of TBG are reduced by about 66% and 45%, respectively. Since the presence of Cl and S can promote the release of alkali metals and the generation of PM_1 during combustion [21,22], it can be inferred that the release of Cl and S during the torrefaction process leads to the less production of alkali metal salts and PM_1 during the combustion process. In comparison with WS, the reduction in the yields of PM_1 of TWS is mainly reflected in the reduction of Na and Cl (Fig. 4c). On the other hand, the contents of Na in WS and TWS have no significant differences, but the contents of Cl and S decrease. The difference is that, compared with WS, the content of Cl of TWS is reduced by less than 10%, which is much lower than the degree of reduction of Cl content in BG torrefaction process. Previous studies have shown that Cl plays a dominant role in the emission of PM_1 if the mole ratio of Cl to S is greater than 2 [23]. So, the reduction in PM_1 from combustion of TWS is not much obvious (Fig. 2). Compared with SD, the Na, Ca and S contents of PM_1 from the combustion of TSD show a downward trend. This is mainly due to the 48% reduction in S content in TSD, which reduces the formation of sodium sulfate and $CaSO_4$. Because the Cl content in SD and TSD and the yields of PM_1 from the combustion are low, it is not obvious in terms of the change of PM_1 generated by SD and TSD.

Compared with BG, WS and SD, the reductions in the yields of PM_{1-10} from the combustion of TBG, TWS and TSD are due to Si, Ca/Ca, Si, Mg, Al, Fe/Ca, Mg, Si reductions, respectively (Figs. 4b, 4d and 4f). It can be found that the main reduced elements in PM_{1-10} from the combustion of torrefied biomass are consistent with the main compositions of corresponding PM_{10+}. Therefore, it is speculated that, compared with the raw biomass, the reductions of PM_{1-10} from torrefied biomass are probably due to the promotion of the coalescence/agglomeration of PM_{1-10} and the migration to PM_{10+} with a larger particle size. In order to verify the possibility of particle coalescence/agglomeration, the morphology and composition of the bulk ash from the combustion of each sample were characterized, and the results are shown in Figs. 6 and 7, respectively. It can be found that there is an obvious phenomenon that several particles in the bulk ash from the combustion of raw and torrefied bagasse and wheat straw coalesce or agglomerate. The compositions of the typical particles show that these particles are generally formed by K/Ca/Fe-rich aluminosilicates. Such particles generally have a relatively lower melting point, and the morphology of their molten spherical shape is also confirmed. For SD and TSD, there are fewer spherical aluminosilicate particles in the bulk ash, but there are a large number of flocculent Ca-rich particles, which is mainly due to the large fraction of Ca in SD and TSD (Fig. 5c). Ca-rich particles, especially CaO, generally have a higher melting point, so the degree of melting and coalescence/agglomeration of the particles from the combustion of SD and TSD is significantly weaker. As a result, compared with SD, the degree of the reduction in the production of PM_{1-10} from the combustion of TSD is small (Fig. 2).

There are two main reasons for the promotion of coalescence/agglomeration between particles from the combustion of torrefied biomass: on the one hand, the release of the alkali metals to PM_1 during torrefied biomass combustion reduces. It leads to an increase in the alkali metal contents in coarse particles, which in turn decreases the melting point of coarse particles and promotes the coalescence/agglomeration between coarse particles, or inhibits the breaking of particles. Han et al. [15] studied the combustion of raw and torrefied rice husk and found that the migration of K from PM_1 to PM_{1+} promoted the coalescence/agglomeration of coarse particles from the combustion of torrefied rice husk. As for TSD which has more obvious contents of Ca, the reduction of S in TSD results in the formation of more Cao and less $CaSO_4$ in the combustion process. Cao can react with Si/Al/O to form aluminosilicate and the aluminosilicate can promote the coalescence/agglomeration between particles. On the other hand, as the ash content of the torrefied biomass increases, the furnace ash concentration increases during combustion, and the probability of collisions between particles increases, which is also conducive to the coalescence/agglomeration between particles and the migration to larger particles.

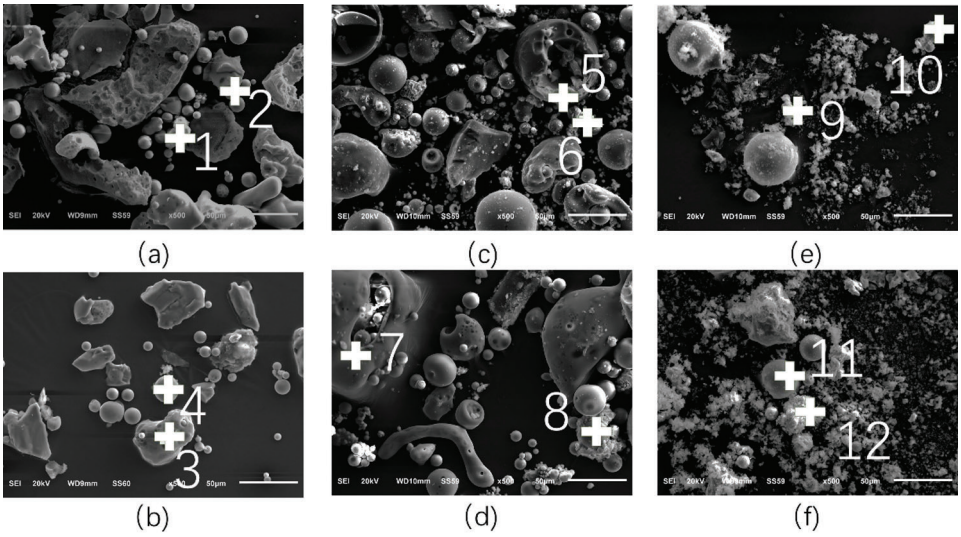

Figure 6: Morphology of bulk ash from combustion. (a) BG, (b) TBG, (c) WS, (d) TWS, (e) SD, (f) TSD

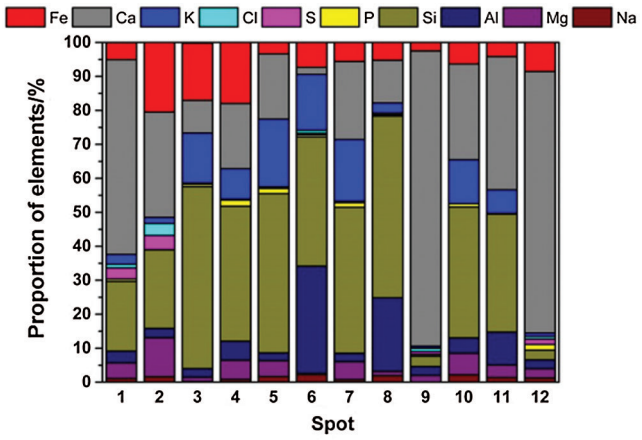

Figure 7: Elemental compositions of typical bulk ash from combustion of different biomasses

4 Conclusion

In this paper, the effects of torrefaction on the emissions of PM_{10} from the combustion of biomass were investigated. The main conclusions are shown as follows:

1) Compared with raw biomass, the moisture and volatile contents of torrefied biomass decrease, but the ash and fixed carbon contents increase. On the other hand, C/H and C/O of torrefied biomass increase and the contents of Cl and S decrease in torrefied biomass;
2) The yields of PM_1 from combustion of torrefied biomass are less than those from combustion of raw biomass, and the degree of PM_1 reduction varies from sample to sample. The main reason is that the Cl and S contents in the torrefied biomass significantly reduce, which leads to less vaporization of alkaline species and emission of PM_1 during combustion;
3) Due to an increase in the alkali metal contents in coarse particles from the combustion of torrefied biomass, the coalescence/agglomeration of coarse particles from the combustion of torrefied biomass can be promoted, which causes PM_{1-10} to migrate to PM_{10+}, thereby reducing the generation of PM_{1-10} from combustion of torrefied biomass.

Acknowledgement: Acknowledgements are also given for the supports from the Analytical and Testing Center at Huazhong University of Science and Technology.

Funding Statement: This research was funded by the National Key Research and Development Program of China (No. 2016YFB0600601).

Conflicts of Interest: The authors declare that they have no conflicts of interest to report regarding the present study.

References

1. Xu, M., Yu, D., Yao, H., Liu, X., Qiao, Y. (2011). Coal combustion-generated aerosols: Formation and properties. *Proceedings of the Combustion Institute, 33(1),* 1681–1697. DOI 10.1016/j.proci.2010.09.014.
2. Wang, W., Wen, C., Chen, L., Liu, T., Li, C. et al. (2020). Effect of combining water washing and carbonisation on the emissions of PM_{10} generated by the combustion of typical herbs. *Fuel Processing Technology, 200,* 106311. DOI 10.1016/j.fuproc.2019.106311.
3. Yang, W., Zhu, Y., Cheng, W., Sang, H., Yang, H. et al. (2017). Characteristics of particulate matter emitted from agricultural biomass combustion. *Energy & Fuels, 31(7),* 7493–7501. DOI 10.1021/acs.energyfuels.7b00229.
4. Qian, C., Li, Q., Zhang, Z., Wang, X., Hu, J. et al. (2020). Prediction of higher heating values of biochar from proximate and ultimate analysis. *Fuel, 265,* 116925. DOI 10.1016/j.fuel.2019.116925.
5. Arias, B., Pevida, C., Fermoso, J., Plaza, M. G., Rubiera, F. et al. (2008). Influence of torrefaction on the grindability and reactivity of woody biomass. *Fuel Processing Technology, 89(2),* 169–175. DOI 10.1016/j.fuproc.2007.09.002.
6. Li, J., Li, Q., Qian, C., Wang, X., Lan, Y. et al. (2019). Volatile organic compounds analysis and characterization on activated biochar prepared from rice husk. *International Journal of Environmental Science and Technology, 16(12),* 7653–7662. DOI 10.1007/s13762-019-02219-4.
7. Uslu, A., Faaij, A. P. C., Bergman, P. C. A. (2008). Pre-treatment technologies, and their effect on international bioenergy supply chain logistics. Techno-economic evaluation of torrefaction, fast pyrolysis and pelletisation. *Energy, 33(8),* 1206–1223. DOI 10.1016/j.energy.2008.03.007.
8. Rousset, P., Aguiar, C., Labbe, N., Commandre, J. (2011). Enhancing the combustible properties of bamboo by torrefaction. *Bioresource Technology, 102(17),* 8225–8231. DOI 10.1016/j.biortech.2011.05.093.
9. Sadaka, S., Negi, S. (2010). Improvements of biomass physical and thermochemical characteristics via torrefaction process. *Environmental Progress & Sustainable Energy, 28(3),* 427–434. DOI 10.1002/ep.10392.
10. Chen, H., Chen, X., Qiao, Z., Liu, H. (2016). Release and transformation characteristics of K and Cl during straw torrefaction and mild pyrolysis. *Fuel, 167,* 31–39. DOI 10.1016/j.fuel.2015.11.059.
11. Saleh, S. B., Flensborg, J. P., Shoulaifar, T. K., Sarossy, Z., Hansen, B. B. et al. (2014). Release of chlorine and sulfur during biomass torrefaction and pyrolysis. *Energy & Fuels, 28(6),* 3738–3746. DOI 10.1021/ef4021262.
12. Khazraie Shoulaifar, T., Demartini, N., Zevenhoven, M., Verhoeff, F., Kiel, J. et al. (2013). Ash-forming matter in torrefied birch wood: Changes in chemical association. *Energy & Fuels, 27(10),* 5684–5690. DOI 10.1021/ef4005175.
13. Wang, W., Wen, C., Li, C., Wang, M., Li, X. et al. (2019). Emission reduction of particulate matter from the combustion of biochar via thermal pre-treatment of torrefaction, slow pyrolysis or hydrothermal carbonisation and its co-combustion with pulverized coal. *Fuel, 240,* 278–288. DOI 10.1016/j.fuel.2018.11.117.
14. Yani, S., Gao, X., Wu, H. (2015). Emission of inorganic PM_{10} from the combustion of torrefied biomass under pulverized-fuel conditions. *Energy & Fuels, 29(2),* 800–807. DOI 10.1021/ef5023237.
15. Han, J., Yu, D., Yu, X., Liu, F., Wu, J. et al. (2019). Effect of the torrefaction on the emission of PM_{10} from combustion of rice husk and its blends with a lignite. *Proceedings of the Combustion Institute, 37(3),* 2733–2740. DOI 10.1016/j.proci.2018.07.011.
16. Mohan, D., Pittman C. U., Steele P. H. (2006). Pyrolysis of wood/biomass for bio-oil: A critical review. *Energy & Fuels, 20(3),* 848–889. DOI 10.1021/ef0502397.

17. Yu, Y., Xu, M., Yao, H., Yu, D., Qiao, Y. et al. (2007). Char characteristics and particulate matter formation during Chinese bituminous coal combustion. *Proceedings of the Combustion Institute, 31(2),* 1947–1954. DOI 10.1016/j.proci.2006.07.116.
18. Gao, X., Wu, H. (2010). Effect of sampling temperature on the properties of inorganic particulate matter collected from biomass combustion in a drop-tube furnace. *Energy & Fuels, 24(8),* 4571–4580. DOI 10.1021/ef100701r.
19. JimÉnez, S., Ballester, J. (2006). Particulate matter formation and emission in the combustion of different pulverized biomass fuels. *Combustion Science and Technology, 178(4),* 655–683. DOI 10.1080/00102200500241248.
20. Garcia-Maraver, A., Zamorano, M., Fernandes, U., Rabacal, M., Costa, M. (2014). Relationship between fuel quality and gaseous and particulate matter emissions in a domestic pellet-fired boiler. *Fuel, 119,* 141–152. DOI 10.1016/j.fuel.2013.11.037.
21. Wang, X., Hu, Z., Adeosun, A., Liu, B., Ruan, R. et al. (2018). Particulate matter emission and K/S/Cl transformation during biomass combustion in an entrained flow reactor. *Journal of the Energy Institute, 91(6),* 835–844. DOI 10.1016/j.joei.2017.10.005.
22. Johansen, J. M., Jakobsen, J. G., Frandsen, F. J., Glarborg, P. (2011). Release of K, Cl, and S during pyrolysis and combustion of high-chlorine biomass. *Energy & Fuels, 25(11),* 4961–4971. DOI 10.1021/ef201098n.
23. Kassman, H., Bäfver, L., Åmand, L. (2010). The importance of SO_2 and SO_3 for sulphation of gaseous KCl–An experimental investigation in a biomass fired CFB boiler. *Combustion and Flame, 157(9),* 1649–1657. DOI 10.1016/j.combustflame.2010.05.012.